GEOPHYSICAL RESEARCH LETTERS, VOL. 34, L07701, doi:10.1029/2006GL028946, 2007

Spatial patterns and fire response of recent Amazonian droughts

Luiz Eduardo O. C. Aragão,[1] Yadvinder Malhi,[1] Rosa Maria Roman-Cuesta,[1] Sassan Saatchi,[2] Liana O. Anderson,[1] and Yosio Edemir Shimabukuro[3]

Received 29 November 2006; revised 12 February 2007; accepted 19 February 2007; published 3 April 2007.

[1] There has been an increasing awareness of the possibility of climate change causing increased drought frequency in Amazonia, with ensuing impacts on ecosystems and human populations. This debate has been brought into focus by the 1997/1998 and 2005 Amazonian droughts. We analysed the spatial extent of these droughts and fire response to the 2005 drought with TRMM and NOAA-12 data, respectively. Both droughts had distinct fingerprints. The 2005 drought was characterized by its intensification throughout the dry season in south-western Amazonia. During 2005 the annual cumulative number of hot pixels in Amazonia increased 33% in relation to the 1999–2005 mean. In the Brazilian state of Acre, at the epicentre of the 2005 drought, the area of leakage forest fires was more than five times greater than the area directly deforested. Fire leakage into flammable forests may be the major agent of biome transformation in the event of increasing drought frequency. **Citation:** Aragão, L. E. O. C., Y. Malhi, R. M. Roman-Cuesta, S. Saatchi, L. O. Anderson, and Y. E. Shimabukuro (2007), Spatial patterns and fire response of recent Amazonian droughts, *Geophys. Res. Lett.*, *34*, L07701, doi:10.1029/2006GL028946.

1. Introduction

[2] The correlation between Amazonian droughts and El Niño events has been previously described [*Marengo*, 1992; *Uvo et al.*, 1998; *Ronchail et al.*, 2002; *Marengo*, 2004], but increased attention has recently focussed on the importance of tropical Atlantic sea surface temperature (SST) anomalies related to the Atlantic Multidecadal Oscillation (AMO) [*Li et al.*, 2006; *Marengo et al.*, 2007], which has been implicated as a causal factor in the drought of 2005 [*Marengo et al.*, 2007]. The two droughts in our study were both induced by SST anomalies: the 1997/1998 drought was caused by a combination of an exceptionally strong El Niño event (warm tropical eastern Pacific) and a positive AMO anomaly (warm tropical North Atlantic) [*Ronchail et al.*, 2002], whereas the 2005 drought was associated only with the positive AMO [*Marengo et al.*, 2007].

[3] Low water availability for plant uptake may have direct impacts on vegetation phenology, physiology, structure and composition of Amazonian forests. In seasonally dry eastern and central Amazonian forests the suppression of tree growth was reported as a response of the intact canopy to drought [*Nepstad et al.*, 2004]. Drought may also increase tree mortality, which becomes more dramatic in the forest edges [*Laurance and Williamson*, 2001]. However, the most drastic drought response is the spread of forest fires. Drought-induced water stress on intact forests is likely to increase leaf shedding, generating leaf litter accumulation and drying, due to increasing canopy openness and understory insolation [*Laurance and Williamson*, 2001]. These conditions associated with intense forest degradation by logging and deforestation can dramatically increase the risk of fires [*Cochrane et al.*, 1999].

[4] Here, we analysed the spatial extent, intensity and impacts of the 1997/1998 and 2005 droughts in terms of anomalies of rainfall and fire frequency, over the Amazonian region using satellite observations. The boundaries of the region were defined according to the definition of [*Eva and Huber*, 2005]. Closed-canopy rainforests are the dominant vegetation type throughout most of this region, covering ~70% of the area.

2. Methods

2.1. Rainfall Datasets

[5] We used a time-series (1998–2005) of the TRMM data (Tropical Rainfall Measuring Mission, 3B43-v6), at 0.25° spatial resolution [*NASA*, 2006]. The cumulative monthly precipitation was estimated in mm month^{-1} considering a 30-day month for all the datasets.

[6] As TRMM data are not available for 1997, a critical time period for droughts in Amazonia, we inferred spatially detailed 1997 TRMM monthly rainfall surfaces by combining the Climate Research Unit (CRU TS 2.0) interpolated ground observation dataset [*Mitchell et al.*, 2004, available at http://www.tyndall.ac.uk/publications/working_papers/wp55.pdf], linearly resampled to 0.25° spatial resolution, and the TRMM mean rainfall data. We first calculated monthly rainfall residuals ($CRU_{residual}$) between the CRU 1997 surface (CRU_{1997}) and the mean CRU surface over the period 1998–2000 ($CRU_{1998-2000}$) for each month separately (equation 1).

$$CRU_{residual}(i,j) = CRU_{1997}(i,j) - CRU_{1998-2000}(i,j) \quad (1)$$

[7] This calculation was repeated for each pixel (i, j) of the surface. The $CRU_{residual}$ was then added to the 1998–2000 TRMM rainfall mean surface ($TRMM_{1998-2000}$) for building the 1997 monthly TRMM rainfall surface ($TRMM_{1997}$) (equation 2).

$$TRMM_{1997}(i,j) = CRU_{residual}(i,j) + TRMM_{1998-2000}(i,j) \quad (2)$$

[1] Environmental Change Institute, Oxford University Centre for the Environment, University of Oxford, Oxford, UK.
[2] Jet Propulsion Laboratory, California Institute of Technology, Pasadena, California, USA.
[3] Brazilian Institute for Space Research, São José dos Campos, Brazil.

0094-8276/07/2006GL028946

[8] This approach assumes that regional variation of the rainfall anomaly can be estimated more robustly from ground observations than regional variation of the mean rainfall, and takes advantage of the detailed spatial information contained in the TRMM dataset.

[9] From this data we estimated the dry season length (DSL) for each pixel, as the number of months with precipitation <100 mm [*Sombroek*, 1966] (see next section for the assumption behind the 100 mm month^{-1} threshold definition).

2.2. Rainfall Anomalies and Cumulative Water Deficits

[10] To quantify the intensity and duration of the drought across Amazonia we calculated rainfall anomalies for 1997, 1998 and 2005 ($TRMM_{anomaly}$) as the departure from the 1998–2005 mean ($TRMM_{1998-2005}$), normalized by the standard deviation (σ). Rainfall surfaces were grouped into trimesters (three-month cumulative rainfall) to enhance seasonal differences. $TRMM_{anomaly}$ was then calculated for each year (y) and each trimester (t) on a pixel-by-pixel basis (equation 3).

$$TRMM_{anomaly,t}(i,j) = \frac{TRMM_{y,t}(i,j) - TRMM_{1998-2005,t}(i,j)}{\sigma_{1998-2005,t}(i,j)} \quad (3)$$

[11] A complementary measure of drought severity is the maximum cumulative water deficit (*MWD*), which corresponds to the maximum value of the accumulated water deficit (*WD*) reached for each pixel within the year. For this, we first calculated the monthly *WDs* based on the approximation that a moist tropical canopy transpires ~100 mm month^{-1}. This value is derived from the mean evapotranspiration obtained by ground measurements in different locations and seasons in Amazonia [*Shuttleworth*, 1989; *Da Rocha et al.*, 2004; *von Randow et al.*, 2004]. Hence, when monthly rainfall is less than 100 mm the forest enters into water deficit. The following rule was applied to calculate the *WD* for each month (n) on a pixel-by-pixel basis, with evapotranspiration (E), fixed at 100 mm month^{-1}:

$$\text{If } WD_{n-1}(i,j) - E(i,j) + P_n(i,j) < 0;$$
$$\text{then } WD_n(i,j) = WD_{n-1}(i,j) - E(i,j) + P_n(i,j);$$
$$\text{else } WD_n(i,j) = 0$$

[12] Subsequently, the *MWD* was obtained for each pixel as the negative of the minimum value of *WD* among all the months in each one of the years. The *MWD* is a useful indicator of "meteorologically-induced" water stress without taking into account local soil conditions and plant adaptations, which are poorly understood in Amazonia.

2.3. TRMM Rainfall Validation

[13] Rainfall data were validated against 11 Amazonian ground stations. We evaluated the 1998–2005 time series separately from generated 1997 values (Table S1 and Figure S1 of the auxiliary material).[1] Ground data were obtained through the ANA (Brazilian Water Agency) database (available at http://hidroweb.ana.gov.br). To minimize geolocation errors, the TRMM rainfall values corresponding to each ground station were extracted using a 3 × 3 pixels window with the ground station located at the central pixel of this window. There is station-by-station variability for both 1998–2005 and 1997 values. TRMM works well for average rainfall <300 mm month^{-1}, but underestimates high rainfall events. For drought periods TRMM tends to overestimate rainfall, and consequently underestimate by up to 40% *WDs* more negative than −300 mm. Much of the observed scatter is likely to come from scale problems, as we are comparing the regional values from TRMM (~5600 km^2) with point measurements from the rain gauges.

2.4. Hot Pixel Anomalies

[14] With the exception of Colombia, hot pixel counts were derived from daily, 1km spatial resolution, NOAA-12 (National Oceanic and Atmospheric Administration) database from the Brazilian Institute for Space Research (INPE) Queimadas project (mid 1998–2005; available at http://www.cptec.inpe.br/queimadas/). Colombian hot pixel data were obtained from the MODIS Rapid Response System (available at http://maps.geog.umd.edu/firms/), monthly accumulated (2001–2005), at 1km spatial resolution. We used NOAA-12 and MODIS thermal anomalies captured in the evenings and morning/afternoon, respectively. Hot pixels are indicators of fires and may well underestimate their occurrence, but hot pixel counts do allow evaluation of anomalous patterns over time. Due to intrinsic hot pixel detection algorithm limitations (see the work by *Giglio et al.* [1999]) and different datasets used, our fire analysis minimized these biases by relying on hot pixel anomalies. The original data were aggregated into monthly-accumulated hot pixels at 0.25° spatial resolution. The trimester hot pixel anomalies were then calculated in terms of hot pixel density (accumulated number of monthly hot pixel counts), similarly to the rainfall data (equation 3). However, we used the 1999–2005 mean, due to missing data in 1998 for NOAA-12 and the 2001–2005 mean for the MODIS data.

[15] To explore the interactions between land use change and climatic conditions on fire patterns during the 2005 drought, we evaluated the case of eastern Acre in greater detail. The INPE DETER (Detection of Deforested Areas in Real Time project) 2004 dataset (available at http://www.obt.inpe.br/deter/dados/) was used to identify land cover types in the study region. We calculated the annual cumulative hot pixel counts from the NOAA-12 thermal anomalies dataset for 2004 and 2005. Eastern Acre held ca. 70% of the total hot pixel counts (3,231 NOAA-12 hot pixel counts) during 2005 in Acre.

3. Results and Discussion

[16] The TRMM mean annual rainfall from 1998 to 2005 (6.0 mm d^{-1}) (Table S2) was within the climatological range (5.5–7.9 mm d^{-1}) [*Marengo*, 2004]. The mean DSL for the studied region was 3.6 months (Table S2).

[17] The spatial patterns and seasonal timing of the two droughts were remarkably different (Figure 1). The extent and duration of 1997/1998 rainfall anomalies were much larger than in 2005, but the decrease in precipitation was concentrated in the wet season. For the 1997/1998 drought,

[1] Auxiliary material data sets are available at ftp://ftp.agu.org/apend/gl/2006gl028946. Other auxiliary material files are in the HTML.

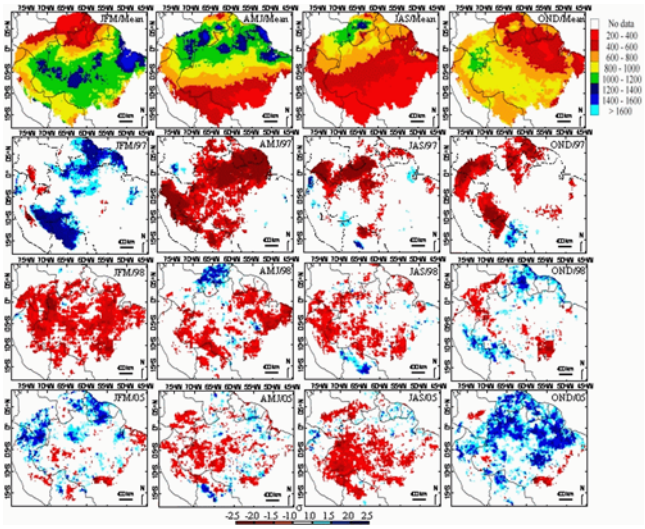

Figure 1. (top row) Average values (1998–2005) for the three-month period cumulative rainfall. Legend is measured in mm. (bottom rows) Rainfall anomalies for the same three-month period in 1997, 1998 and 2005 (see main text). The units are the anomalies normalized by the standard deviation (σ) of the time-series (1998–2005) for each pixel.

the largest negative rainfall anomalies (between 1.0 σ and 2.5 σ) were observed in April-May-June (AMJ) of 1997 during the wet-to-dry season transition for most of Amazonia and January-February-March (JFM) of 1998, during the wet season for most of Amazonia except the far north. In contrast, 2005 showed a redistribution of rainfall patterns, with increased rainfall in the wet season in the north-east and decreased rainfall in dry season in the west. The negative anomalies intensified only during AMJ (early dry season), and peaked in July-August-September (JAS) (dry season). El Niño-caused rainfall anomalies tend to be focussed on northern Amazonia [*Malhi and Wright*, 2004; *Marengo et al.*, 2007]. The broader spatial extent of the 1997/1998 anomalies suggests that the warm tropical north Atlantic was influential in suppressing rainfall in southern Amazonia, at the same time that the El Niño was affecting rainfall in the north [*Marengo et al.*, 2007].

[18] In contrast to 1997/1998, the 2005 drought did not affect the basin-wide total annual rainfall (Table S2). However, the mean *MWD* for 2005 was 37% larger than the long-term mean and was comparable to the intense *MWD* recorded in 1997 (Table S2). The spatial pattern and particularly the timing of the 2005 rainfall anomalies led to an extensive drought. Figure 2 shows the patterns of *MWDs* for 1997, 1998 and 2005. During the 2005 drought an area of more than 3,300,000 km^2 experienced enhanced water stress (48% of the basin) and 5% (160,000 km^2) of the affected area had an enhancement of peak water deficits by more than 200 mm. These values are comparable to the 1997/1998 drought, when 63% of the Amazon basin (4,310,000 km^2) was under enhanced water stress and 10% (387,000 km^2) of the water deficits were enhanced by more than 200 mm. North-western Amazonia has such high monthly rainfall rates and small *WDs* (Figure 2, bottom right) that even strongly negative precipitation anomalies do not induce widespread water stress. The epicentre of the 1997/1998 drought anomaly was northern and far north-western Amazonia, a region which is out of phase with most of Amazonia and experiences its dry season in January-March, coinciding with the peak negative rainfall anomaly of 1997/1998. By contrast, the epicentre of the 2005 event was in south-western Amazonia. In both cases the most impacted regions were where the timing of the negative precipitation anomaly converted a moderate dry season into an intense one.

[19] Some GCM predictions point to a higher frequency of AMO induced droughts over the 21st century [*Li et al.*, 2006]. Our analysis suggests that the most vulnerable region in these circumstances stretches across southern Amazonia, with a particular focus in south-western areas (states of Madre de Dios (Peru), Acre (Brazil) and Pando (Bolivia)). In contrast, the most vulnerable region during El Niño droughts is in northern and north-eastern Amazonia.

[20] During the 2005 drought the cumulative number of hot pixels in Amazonia increased 33% in relation to the 1999–2005 mean, while, according to the PRODES data (Assessment of Deforestation in Brazilian Amazonia) from INPE (available at http://www.obt.inpe.br/prodes/index.html), deforestation in the Brazilian Amazon was 13% lower than the mean between 1999–2005 (Figure S2a). Land conversion through deforestation and subsequent activities is one of the main drivers of the fire dynamics in Amazonia [*Uhl and Kauffman*, 1990]. However, our analysis demonstrates that drought increases forest flammability and fire extent even in the presence of declining deforestation. Note that PRODES deforestation data for a single year are quantified as the cumulative deforestation from August from the previous year to August from the current year, but dates are not fixed because of the availability of cloud-free images (INPE/PRODES). However, more than 80% of annual deforestation occurs between January and August (INPE/DETER), and hence the comparison between deforestation figures and hot pixel counts is largely valid.

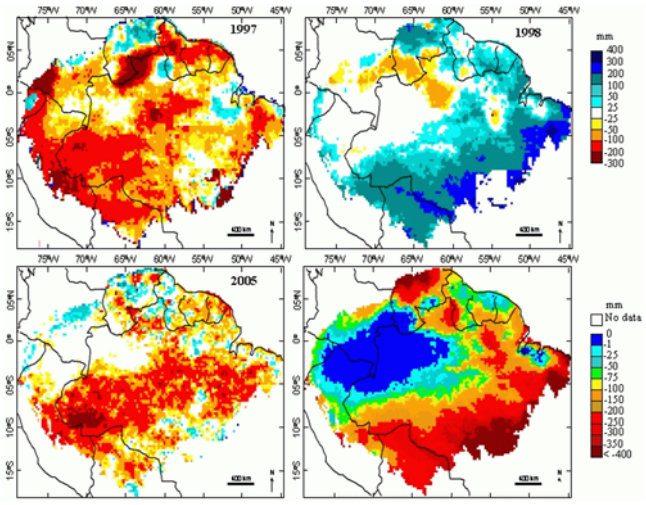

Figure 2. Maximum cumulative water deficit (*MWD*) anomaly for (top left) 1997, (top right) 1998, and (bottom left) 2005 as estimated by TRMM and CRU data (1997) in relation to (bottom right) the mean *MWD* from the period between 1998–2005. Top legend corresponds to the *MWD* anomaly (mm) and bottom legend to the mean *MWD* (mm). Negative values indicate enhanced water stress and positive values indicate reduced water stress.

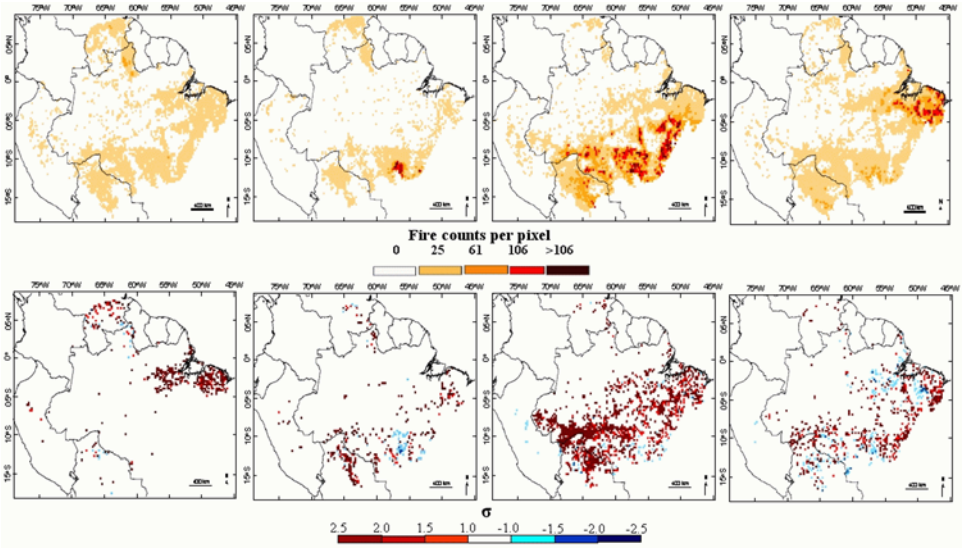

Figure 3. (top) Mean values for the three-month period cumulative hot pixel counts derived from NOAA-12 (1999–2005) and MODIS (2001–2005), and (bottom) hot pixel anomalies for the same three-month period. The anomalies are normalized by the standard deviation (σ) of the time-series for each pixel (spatial resolution 0.25°).

[21] In 2005 fire frequency increased in the drought-affected region (Figure 3), as long as there were human settlements to act as ignition sources. Fire peaked in well-known land conversion areas, such as the "arc of deforestation" in Brazil and northern Bolivia. Despite similar drought anomalies, fire incidence was much higher in Acre and northern Bolivia, which are foci of land use change, than in south-eastern Peru, which currently has little road infrastructure. Throughout JAS period, following the dry season cycle in Amazonia (Figure 1, top row), notable fire anomalies (>1 σ) covered areas from the southwest and south to the eastern region of the basin in agreement with the rainfall anomalies and *MWDs* during 2005. The pattern observed in 2005 was different from that observed during the El Niño drought in 1997/1998 where the most critical region was northern Amazonia [*Cochrane and Schulze*, 1998].

[22] Our analysis points to a critical region located in south-western Amazonia with the largest *WD*s >200 mm and fire anomalies >1.5 σ in 2005. The conjunction of severe drought and ignition sources from human activities was responsible for 6,500 km^2 of burned land surface area in Acre in 2005, of which 3,700 km^2 were in previously deforested areas and 2,800 km^2 corresponded to forest fires [*Shimabukuro et al.*, 2006]. Simultaneously, the rate of deforestation in Acre State decreased by 30% between 2004 (769 km^2) and 2005 (541 km^2) (INPE/PRODES). The total area of burnt forests in 2005 was hence five times greater than the deforested area. These burnt forests are likely to be much more vulnerable to further burns if the drought were to reoccur soon [*Cochrane et al.*, 1999].

[23] Our study case showed that under the drought conditions of 2005, the total hot pixel count increased by 376% in eastern Acre in comparison to 2004 and the hot pixel counts within forest regions increased by 280% from 2004 (286 counts) to 2005 (1086 counts). In contrast, deforestation within this region decreased 16% from 2005 to 2004 (INPE/PRODES). Most of the hot pixel counts for forests in 2005 fell within the edge of mapped burn scars [*Shimabukuro et al.*, 2006], in forests close to already deforested regions (Figure S2b). This result indicates that the burn scars map is able to show areas affected by ground and under-canopy forest fires, due to the post-fire vegetation responses, that are not detectable by hot pixel detection algorithms.

4. Conclusions

[24] Our analysis is focussed on two droughts, each caused by a particular constellation of climatological variables. Nevertheless, they are useful in identifying which regions of Amazonian forest are most vulnerable to increased drought incidence. ENSO-associated droughts have a greater impact in northern, central and eastern Amazonia. AMO-associated droughts cause precipitation anomalies mainly in western Amazonia during the dry season. However, because NW Amazonia has inherently high background rates of precipitation, hydrological stresses are particularly focused in SW Amazonia. A combination of Eastern Pacific and tropical North Atlantic warming could affect wide swathes of Amazonia. In the event of increased drought frequency, the leakage of fires from forested areas, is likely to be the major agent of forest transition, rather than changes in forest ecology and physiology. If tropical North Atlantic warming becomes a dominant mode under 21st century climate change, as predicted by some models [*Li et al.*, 2006], south-western Amazonia may be a region particularly vulnerable to forest dieback. This situation would be particularly exacerbated by the expansion of fire ignition sources, such as the planned Brazil-Peru connecting highway in SW Amazonia [*Soares-Filho et al.*, 2006].

[25] **Acknowledgments.** The data used in this study were acquired as part of the TRMM project jointly sponsored by the Japan National Space Development Agency (NASDA) and the U.S. National Aeronautics and Space Administration (NASA) Office of Earth Sciences. We thank the INPE PRODES and DETER programs and ANA for making their data and images freely available. This work was supported by an Natural Environment Research Council Urgency Grant (NE/D01025X/1).

References

Cochrane, M. A., and M. D. Schulze (1998), Forest fires in the Brazilian Amazon, *Conserv. Biol.*, *12*, 948–950.

Cochrane, M. A., et al. (1999), Positive feedback in the fire dynamic of closed canopy tropical forests, *Science*, *284*, 1832–1835.

Da Rocha, H. R., et al. (2004), Seasonality of water and heat fluxes over a tropical forest in eastern Amazonia, *Ecol. Appl.*, *14*, S22–S32.

Eva, H. D., and O. Huber (Eds.) (2005), A proposal for defining the geographical boundaries of Amazonia, *Rep. EUR 21808-EN*, Off. Publ. Eur. Communities, Luxembourg.

Giglio, L., J. D. Kendall, and C. O. Justice (1999), Evaluation of global fire detection algorithms using simulated AVHRR infrared data, *Int. J. Remote Sens.*, *20*, 1947–1985.

Laurance, W. F., and G. B. Williamson (2001), Positive feedbacks among forest fragmentation, drought, and climate change in the Amazon, *Conserv. Biol.*, *15*, 1529–1535.

Li, W., R. Fu, and R. E. Dickinson (2006), Rainfall and its seasonality over the Amazon in the 21st century as assessed by the coupled models for the IPCC AR4, *J. Geophys. Res.*, *111*, D02111, doi:10.1029/2005JD006355.

Malhi, Y., and J. Wright (2004), Spatial patterns and recent trends in the climate of tropical rainforest region, *Philos. Trans. R. Soc. London, Ser. B*, *359*, 311–329.

Marengo, J. A. (1992), Interannual variability of surface climate in the Amazon basin, *Int. J. Climatol.*, *12*, 853–863.

Marengo, J. A. (2004), Interdecadal variability and trends of rainfall across the Amazon basin, *Theor. Appl. Climatol.*, *78*, 79–96.

Marengo, J. A., et al. (2007), The drought of Amazonia in 2005, *J. Clim*, in press.

Mitchell, T. D., T. R. Carter, P. D. Jones, M. Hulme, and M. New (2004), A comprehensive set of high-resolution grids of monthly climate for Europe and the globe: The observed record (1901–2000) and 16 scenarios (2001–2100), *Working Pap. 55*, Tyndall Cent., Norwich, UK.

NASA (2006), Monthly 0.25° × 0.25° TRMM and other sources rainfall, http://disc.gsfc.nasa.gov/data/datapool/TRMM_DP/01_Data_Products/02_Gridded/07_Monthly_Other_Data_Source_3B_43/, NASA Distrib. Active Arch. Cent., Goddard Space Flight Cent. Earth Sci., Greenbelt, Md.

Nepstad, D., et al. (2004), Amazon drought and its implications for forest flammability and tree growth: A basin-wide analysis, *Global Change Biol.*, *10*, 704–717, doi:10.1111/J.1529-8817.2003.00772.x.

Ronchail, J., et al. (2002), Interannual rainfall variability in the Amazon basin and sea-surface temperatures in the equatorial Pacific and the tropical Atlantic Oceans, *Int. J. Climatol.*, *22*, 1663–1686.

Shimabukuro, Y. E., V. Duarte, E. Arai, R. M. de Freitas, D. M. Valeriano, I. F. Brown, M. L. R. Maldonado (2006), Fraction images derived from Terra MODIS data for mapping burned area in Acre State, Brazilian Amazonia, paper presented at IEEE International Geoscience and Remote Sensing Symposium, Denver, Colo., 31 July to 4 Aug.

Shuttleworth, W. J. (1989), Micrometeorology of temperate and tropical forest, *Philos. Trans. R. Soc. London, Ser. B*, *324*, 299–334.

Soares-Filho, B. S., et al. (2006), Modelling conservation in the Amazon basin, *Nature*, *440*, 520–523.

Sombroek, W. G. (1966), *Amazon Soils*, 303 pp., Cent. for Agric. Publ. and Doc., Wageningen, Netherlands.

Uhl, C., and B. Kauffman (1990), Deforestation, fire susceptibility, and potential tree responses to fire in the eastern Amazon, *Ecology*, *7*(2), 437–449.

Uvo, C. B., C. A. Repelli, S. E. Zebiak, and Y. Kushnir (1998), The relationships between tropical Pacific and Atlantic SST and northeast Brazil monthly precipitation, *J. Clim.*, *11*, 551–562.

von Randow, C., et al. (2004), Comparative measurements and seasonal variations in energy and carbon exchange over forest and pasture in south west Amazonia, *Theor. Appl. Climatol.*, *78*, 5–26.

L. O. Anderson, L. E. O. C. Aragão, Y. Malhi, and R. M. Roman-Cuesta, Environmental Change Institute, Oxford University Centre for the Environment, University of Oxford, South Parks Road, Oxford OX1 3QY, UK. (laragao@ouce.ox.ac.uk)

S. Saatchi, Jet Propulsion Laboratory, California Institute of Technology, Pasadena, CA 91109, USA.

Y. E. Shimabukuro, Brazilian Institute for Space Research, São José dos Campos 12227-010, Brazil.